Biomass Conversion and Biorefinery (2023) 13:10853–10863
https://doi.org/10.1007/s13399-021-01990-0

ORIGINAL ARTICLE

Photocatalytic degradation of methylene blue dye and fungi *Fusarium equiseti* using titanium dioxide recovered from drinking water treatment sludge

Santhana Krishnan[1] · Nor Syahidah Zulkapli[1] · Mohd Fadhil Bin Md Din[1] · Zaiton Abd Majid[2] · Mohd Nasrullah[3] · Fadzlin Md Sairan[1]

Received: 25 June 2021 / Revised: 21 September 2021 / Accepted: 22 September 2021 / Published online: 28 September 2021

Abstract

Massive amount of water treatment sludge is produced annually and majorly being treated via landfills which will eventually lead to the environmental problem. In this study, an attempt was made to evaluate the photocatalytic activity of titanium dioxide (TiO_2) that was extracted from drinking water treatment plant sludge (DWTP) against methylene blue dye and fungi *Fusarium equiseti.* The TiO_2 as white precipitate was formed at pH 6 using solvent extraction methods and further characterized using X-ray fluorescence (XRF), X-ray diffraction (XRD), and field emission scanning electron microscope (FESEM). Photocatalytic degradation of methylene blue solution by TiO_2 was conducted in a closed home built-photocatalytic reactor. The effect of irradiation time, amount of loaded catalyst (TiO_2) on the degradation of methylene blue and inhibition of *F. equiseti* were also investigated, respectively. The fungi *F. equiseti* was isolated and screened using polymerase chain reaction (PCR) with 100% identities. Results revealed that a maximum of 86% methylene blue degradation was achieved at 4-h reaction time with the 0.5 g/L of TiO_2-loaded catalyst and 50% inhibition of the *F. equiseti* after 14 days. This work provides new insight into the TiO_2 recovery from alternative resources and TiO_2 as a high performance catalyst and facilitates its application in photocatalytic degradation of organic compounds.

Keywords Dye removal · Fungal inhibition · Photo catalyst · Titanium dioxide · Waste recovery

1 Introduction

Current emphasis on the industrialization and rapid growth of technology has led to high demand of titanium [1]. The most widely used titanium product, titanium dioxide (TiO_2) belongs to the family of transition metal oxides, has excellent photocatalytic property, low toxicity, and high chemically stable [2]. Due to the high refractive index, TiO_2 is extensively used as the reflective pigment in coating materials. This coating is designed to achieve high reflectance of solar radiation thus mitigating the heat transfer to the interior of the coated material. TiO_2 is highly relevant for a host of industrial applications in environmental, synthetic textiles, packaging, health care, and medical care products [3]. Research on photocatalytic degradation of organic pollutants and microorganisms has been in continuous expansion in recent decades and TiO_2 is still by far the most used photocatalyst [4]. For example, dyes are an important source in various industries such as textile, leather, paint, food, cosmetic, and paper industries. More than thousand dyes have been classified as textile dyes which are used to color variety of fabrics [5]. Methylene blue is a cationic dye which mostly used in industry as colorant, but the waste of this industry also contains about 20 % dye and therefore, disposal of industrial effluents into water bodies cause water pollution and with human health [6]. TiO_2 offers notable

✉ Santhana Krishnan
kcsanthana@utm.my

✉ Mohd Fadhil Bin Md Din
mfadhil@utm.my

[1] Centre for Environmental Sustainability and Water Security (IPASA), Research Institute of Sustainable Environment (RISE), School of Civil Engineering, Faculty of Engineering, Universiti Teknologi Malaysia (UTM), 81310 Skudai, Malaysia

[2] Department of Chemistry, Faculty of Science, Universiti Teknologi Malaysia (UTM), 81310 Skudai, Malaysia

[3] Faculty of Civil Engineering Technology, Universiti Malaysia Pahang (UMP), Gambang, Malaysia

remediation potential, economic feasibility, and high efficiency for removal of organic pollutants. However, the dye degradation/remediation can be affected by various factors viz. pH, temperature, dye concentration, irradiation time, catalyst concentration, etc. An optimization study is necessary for the development of industrial-scale treatment plants [7]. Optimization of as time, pH, dye concentration, temperature, and biosorbent dosage during the biosorption of malachite green dye from aquatic systems by nano zero valent iron-stacked-activated carbon influenced the Langmuir adsorption capacity of 187.3 mg/g. The procedure seemed to be non-toxic, potential to retain biosorbent from the solution, applicable for multiple cycles [8].

The photocatalytic property of TiO_2 has made itself among the best agent in killing, or inhibits the growth of microorganisms such as bacteria, fungi, and algae [9]. Zhu et al. [10] had investigated the antibacterial activity of the synthesized TiO_2 nanoparticles against several types of species of bacteria and out of all species, *Staphylococcus aureus* and *Streptococcus pyogenes* were successfully inhibited. Malaysia is one of the tropical climate and humid country which is likely to possess an esthetic biodeterioration due to microbial colonization. The construction materials such as wallpaper, wood-based materials, ceiling boards, glass wool, and plaster are prone to the development of mould due to the organic content [11]. Fusarium genus is a filamentous fungus commonly found in soil and it can be worldwide spread through water. Previous contributions showed that Fusarium is a good model phytopathogen due to its high resistance to standard water disinfection practices and its negative effect on humans [12]. There is an increasing interest in the making of hygienic coating, which would minimize the transmission of microorganism infection, avoiding human health risks and having an important economic impact [13]. Saravanan et al. [14] experimented on the immobilized *Aspergillus niger* and *Aspergillus flavus* biomass for the simultaneous removal of Cu(II) ion and Reactive Green 6 dye from aqueous phase. The factors influencing biosorption process inferred optimal values of 25 mg/L of adsorbate with equilibrium time of 60 min, 2.5 g of immobilized fungal biomass, temperature of 303 K, and pH of 5.0 for the maximal removal of pollutants.

Until date, hydrometallurgical route is one of the most favorable conventional processes used to recover the titanium. It is basically a metal processing technology that uses a chemical process combining water, oxygen, or other substances in a pressurized or other vessel to dissolve metal from its ore. This technique mainly requires two distinct stage namely leaching (solid-liquid extraction) and purification process [15]. Until the recent past, titanium recovery from the low-grade ores and wastes had been widely practiced to overcome the exhausted of this natural resource. For instances, the titanium recovery from industrial slag [16] red mud [17], Langkawi black sand [18] are among others. It is known that aluminum, silica, and iron are among the major constituent exists in the drinking water treatment plant (DWTP) sludge. Interestingly, our current findings reveal the existence of another valuable metal in the DWTP sludge, which is titanium. On a global scale, available literature estimates that 10, 000 tons of sludge is produced daily in most municipalities worldwide and directly disposed to a landfill [15]. DWTP sludge is classified as a scheduled waste due to the high content of aluminum and their characteristic is greatly influenced by the quality of the source of raw water, type of coagulant used, and the water treatment system. The quantity of contaminants or hazardous substances in the DWTP sludge is relatively low, since the clean water resources are preferentially used for domestic purposes [19].

Based on the literature study, there is a limited work on the recovery of TiO_2 using pyrometallurgical technique and biometallurgical technique. Therefore, the re-utilization of DWTP sludge as one of the potential TiO_2 recovery sources using hydrometallurgical route was investigated in our previous study [15]. In that study, optimization on the independent variables was performed with a wide range of factor for the optimal recovery of TiO_2 from the DWTP sludge using response surface methods (RSM). Accordingly, in the present study, the recovered TiO_2 from the DWTP sludge was further purified using anionic extractants (Cyanex 272) and then titanium stripped using hydrochloric acid and precipitate out using light magnesium oxide. The final product TiO_2 was further characterized using XRF, XRD, and FESEM to determine the elemental composition and to confirm the right formation of desired TiO_2. Finally, the photocatalytic activity of extracted TiO_2 was investigated against organic dyes (methylene blue) and also for the isolated fungal stain *Fusarium equiseti*. Methylene blue as a cationic dye was employed to determine the exact effect of irradiation time, and amount of loaded catalyst, on the photoactivity of the extracted TiO_2. The disinfection ability of the TiO_2 was studied using the fungal stain *F. equiseti*. Photocatalytic application can provide solutions for many of the environmental challenges as most of the organic pollutants will undergo degradation to produce less harmful or non-harmful substances under UV light irradiation.

2 Materials and methods

2.1 Sampling

Drinking water treatment plant (DWTP) sludge was collected from Semangar Water Treatment Plant, Kota Tinggi. Alum (liquid aluminum sulfate) and polymer (Nalclear8173 PULV) were used as the coagulant and coagulant aid accordingly. In order to adjust the raw water pH to the desired pH, hydrated lime was used.

2.2 Solvent extraction and characterization studies

In our previous study, titanium was recovered from the DWTP residue and optimized for various factors by acid leaching methods were reported [15]. In continuation, the solvent extraction of titanium from the leaching solution was conducted using 60% Cyanex 272 solvent. Then, stripping process was conducted (organic phase obtained from optimal solvent extraction with Cyanex 272) using 3M HCl at 1:1 organic to aqueous ratio, 29.5 ± 0.5 °C for 30 min. At pH 6.0, the precipitation was complete and a white gelatinous precipitate was obtained as seen in the Fig. 1. After precipitation and calcination, it was found that the precipitate presence in the brownish-white color powder form known as TiO_2. The purified product TiO_2 was further characterized as the analysis on the major oxides present was performed using Bruker S4 Pioneer X-ray fluorescence (XRF) spectrometer. The mineralogical composition was analyzed using X-ray diffraction (XRD) on a Bruker Advance D8 diffractometer with transmission Kα Cu radiation with λ= 1.54045 Å. The surface morphology was observed using field emission scanning electron microscopy (FESEM) at higher magnification with 5.0 kV scanning voltage.

2.3 Photocatalytic degradation of methylene blue by TiO_2

Photocatalytic degradation of methylene blue solution by TiO_2 obtained was conducted in a closed home-built photocatalytic reactor in order to prevent the exposure of the UV light to the surrounding. As shown in Fig. 2, the reactor was made of the box with 40 cm height, length, and width. Magnetic stirrer was placed inside the reactor box

Fig. 1 Final product of recovered TiO_2

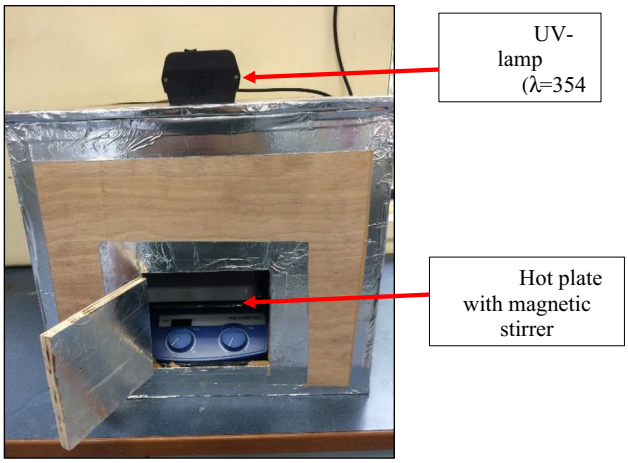

Fig. 2 Home built-photocatalytic reactor

while the UV lamp was placed on top of the box. About 10 ppm of MB stock solution was prepared by weighing 0.01 g of MB powder into a 1-L aluminum wrapped volumetric flask and dissolved with distilled water until reaching the mark level. The solution was stirred for 1 h to obtain a homogenous MB stock solution. After completing the stirring process, 250 mL of stock solution was then transferred into a beaker and placed into the UV box for 4 h. The photocatalytic studies were carried out under λ = 354 nm UV light at room temperature for 4 h. MB solution was first magnetically stirred for 30 min in the dark to reach the adsorption equilibrium throughout the experiment before UV irradiation. Five milliliters of each MB solution were drawn from the beaker using a 0.45-µm filter syringe before a reaction and every 1 h upon the complete reaction. The concentration of the MB solution was analyzed using UV/Vis spectrophotometer. The TiO_2 dosage were range from 0.1 to 1.0 g/L (0.1 g/L, 0.3 g/L, 0.5 g/L, and 1.0 g/L). The suspension was stirred at a controllable speed. After a 4-h irradiation of light, 5 mL of solution were collected using a filter syringe (Nylon, 0.45 µm) and analyzed using UV-Vis spectrophotometer (Perkin Elmer Lambda 25). The efficiency of photo-degradation was determined as % degradation. Equation 1 was used to calculate the percentage of MB degradation:

$$\text{Degradation of methylene blue } (\%) = \frac{C0 - Ct}{C0} \times 100 \quad (1)$$

where
C_0 = initial concentration of sample (ppm)
Ct = concentration of sample at certain time (ppm)

2.4 Photocatalytic degradation of fungi by TiO_2

The fungi were inoculated using the potato dextrose agar (PDA) and all the cultured fungi were stored in the cupboard for 7 days. The characterization of the fungi sample was done via a PCR analysis. PDA medium containing TiO_2 was prepared by adding an amount of TiO_2 in distilled water (0.5 g/L) into agar solution and both were solidified together. A disc (1.4 cm) of mycelial material was taken from the edge of 7-day-old fungal cultures and placed on the new dish (sample test) using a cork borer. The observation of fungi growth in PDA medium containing TiO_2 was made in the duration of 14 days. The effect of UV was conducted in the photoreactor box with a source of UV light supplied for 4 h per day.

2.5 Polymerized chain reaction (PCR analysis)

The PCR analysis was conducted to identify the species of isolated fungi. The DNA of the fungal tissue body was extracted using a Wizard® Genomic DNA Purification Kit (Promega, USA, Cat No: A1120). The polymerase chain reaction was performed as follows: 1 cycle at 94 °C for 2 min, 25 cycles at 94 °C for 35 s, 50 °C for 30 s, and 72 °C for 3 min and ended with 1 cycle at 72 °C for 10 min. The sequence was compared with other 18S rDNA and internal transcribed spacer (ITS) region sequences that were obtained from Basic Local Alignment Search Tool (Blast) on the National Center for Biotechnology (NCBI) server (http://blast.ncbi.nlm.nih.gov/Blast.cgi). The phylogenetic examination with other firmly related grouping was done trailed by various succession arrangements utilizing the program MUSCLE 3.7. The precise phylogenetic investigation was performed utilizing the program PhyML 3.0.

3 Results and discussions

3.1 Solvent extraction and stripping

Toluene was used as the organic diluent due to high solubility in organophosphorus extractant. In these separation, Ti(IV) was extracted into the organic phase leaving the unwanted metal ions in aqueous phase. It can be observed from the results that Ti(IV), Al(III) along with the traces of Fe(III) were extracted into the organic phase leaving behind the other metal ions in aqueous solution. The results indicated that the extraction efficiency of metals follows the order of titanium > aluminum > iron for Cyanex 272. Cyanex 272 had shown higher selectivity particularly on the Ti extraction from the leaching solution with 86.2%. Cyanex 272 or bis (2,4,4-trimethylpentyl) phosphoric acid has proven to be a good extractant for titanium, as well as for cobalt and nickel [20]. However, there have been very few studies on titanium extraction by Cyanex 272 from a mixed metals system with sulfate medium. At the end of the solvent extraction (SX) process, the organic extractant (Cyanex 272) formed two phases in contact with water to carry out the stripping experiments with an aqueous phase. Stripping or back-extraction is generally used for the redistribution of metal ions that are readily present in an organic phase to an aqueous phase. Stripping process or known as back-extraction was conducted using the organic phase obtained from solvent extraction with Cyanex 272 at 60% concentration. In acidic medium, the chloride solutions (stripping agent) were stable because of the negative surface charge, which stabilizes particles toward the agglomeration. Upon the addition of MgO powder, the surface charge was gradually disappeared and the particles start forming aggregates. It is noted that SX has been incorporated into processes to separate titanium from iron and other impurities. The hydrolysis and condensation reactions started immediately as indicated by the rapid increase in turbidity and the formation of visible flocs, which precipitated at the bottom of the flask. At pH=6.0, the precipitation was complete and a white gelatinous precipitate was obtained. After precipitation and calcination, it was found that the precipitate presence in the brownish-white color powder form known as TiO_2. The existence of Fe^{3+} reduces the purity of TiO_2, thus affecting the whiteness of the product. The end product was further characterized and clarified via XRF, XRD, and FESEM analysis. Much work has been done on the separation of valuable metals from the leach solution of various kind of wastes. Gao et al. [21], in his finding, stated higher amount of metals been separated using the SX technique than selective precipitation with sodium hydroxide. SX introduces an organic solvent to the leaching solution where the desired metal ion will dissolve preferably in the organic solvent. In order to enhance the dissolution of metal oxides in an acid reagent, the solubility of the metal ions in the organic solvent must be higher than in the leaching solution [22].

3.2 Characterization of TiO_2

Apparently, DWTP residue is classified as the coagulant, natural, groundwater and manganese residuals [23]. Among these, coagulant residuals constitute the majority of water treatment plant by-products. The production of drinking water comprises the steps of coagulation and flocculation of suspended solids by adding aluminum sulfate as the primary coagulant, ferric salts and polymer [24]. The main components of DWTP residue are clay minerals, fine-grained minerals (mainly oxides and hydroxides of aluminum, titanium and iron), organic matter, and sediment where their characteristics depend on the source of raw water, type of coagulant used, and overall system of treatment plant [25]. It

contains various ranges of valuable oxide components which make it more significant to be used in further applications. According to Gomes et al. [26], the metal composition (% wt.) of DWTP residue consists of Sio_2 54.1%, Al_20_3 28.84, Fe_2CO_3 9.92, Cao 3.1, MgO 0.64, TiO_2 1.28 %wt.

The compounds extracted from drinking water treatment sludge (DWTP) had been analyzed by using XRF. The purity of the recovered TiO_2 with respect to other impurities was around 70.8%. Table 1 shows the XRF analysis of metal oxide composition presence in the final product. It was estimated that the final ratio of TiO_2:Al_2O_3:Fe_2O_3 was 81:11:8 accordingly. The separation of remaining metals, Al and Fe from product containing Ti, were difficult due to their close boiling points.

The X-ray diffraction data of the precipitates obtained under the experimental conditions mentioned above, after drying and calcining is shown in Fig. 3. The characteristic diffraction peaks at 25.3°, 37.8°, 48.0° (2Θ values) indicates that the diffraction pattern corresponds to the crystallized anatase phase. The final precipitate formed was calcined at 550°C as a further increase in the calcination temperature from 700 up to 1000°C would trigger the formation of rutile phase [27]. XRD analysis showed six distinct diffraction peaks which attributed to the TiO_2 anatase phase, Fe_2O_3 hematite, and Al_2O_3. The anatase phase shows greater photocatalytic activity than the rutile phase, but the TiO_2 powder with both anatase and rutile phases shows a much greater photocatalytic activity than the pure anatase powder or the pure rutile powder because of the effect of the rutile phase [27]. All the diffraction peaks are in agreement with the reported data in JCPDS Card File No. 21-1272.

FESEM has been utilized to visualize the surface topology and structure of TiO_2. The FESEM image of recovered TiO_2 is depicted in Fig. 4. The produced agglomerates were randomly oriented due to the difference in the crystalline structures of TiO_2, Fe_2O_3, and Al_2O_3. The micrometer-sized grain aggregates presence in the form of uniformed spherical shape made up with several nanoballs, with considerable variation of particle size which contributes to enhance the active surface area.

3.3 Photo-degradation of methylene blue

The use of TiO_2 has been recognized as a proficient advanced oxidation process and versatile because of its ability to produce reactive oxidative species (like O2− and •OH, ROS) which is highly desired for photocatalytic degradation of organic pollutants and dyes [28]. Photo-degradation of methylene blue under UV light was performed to investigate the photocatalytic activity of TiO_2. The effect

Table 1 XRF analysis of final product TiO_2

Component	TiO_2	Al_2O_3	Fe_2O_3	MgO	NaO	SO_3
Composition (wt. %)	70.78	9.81	6.76	4.59	3.51	3.93

Al_2O_3, aluminum oxide; *Fe_2O_3*, iron oxide; *MgO*, magnesium oxide; *Nao*, sodium oxide; *SO_3*, sulfur trioxide

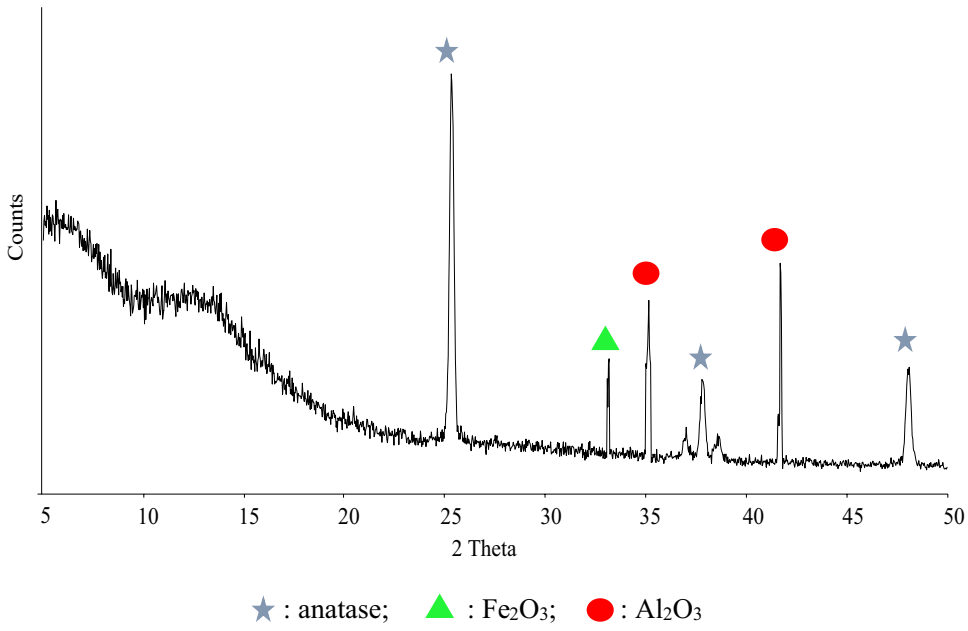

Fig. 3 Diffractogram of final product of TiO_2 precipitate

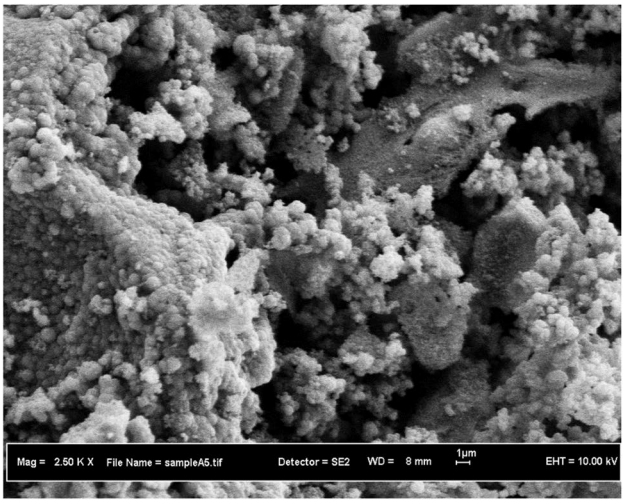

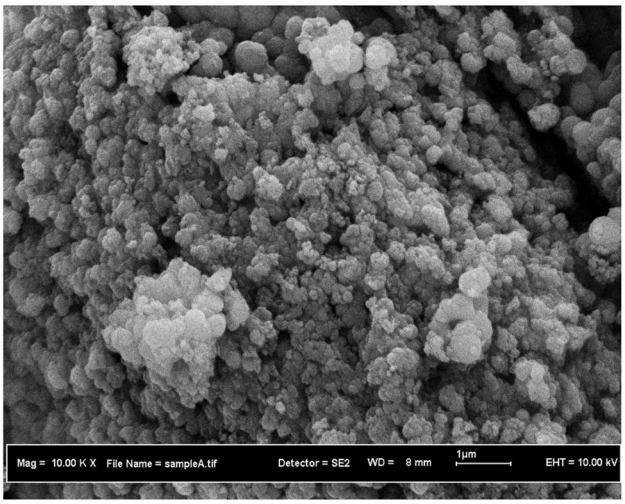

Fig. 4 FESEM image of final product of TiO_2 precipitate

of UV irradiation, amount of TiO_2 loading, and irradiation time on the photo-degradation of methylene blue also were studied. The calibration curves of methylene blue solution were at 2 ppm, 4 ppm, 6 ppm, 8 ppm, and 10 ppm. The maximum absorbance (*A* value) was obtained at wavelength 645 nm. The value of maximum absorbance obtained was in agreement with the previously published reports by Le et al. [29] and Wang et al. [23]. Alakhras et al. [30] have reported photocatalytic experiments and noted that Zeo-TiO_2 mixture gives best result in photocatalytic performance on degradation of Rhodamine B dye than Zeo-ZnO composites under UV radiation. Zeo-TiO_2 catalyst has excellent recycling stability. The common dye pollutants responsible for environmental pollution and their possible remediation via photocatalyst such as TiO_2 coupling with microbial fuel cell (MFC) [31]. In MFC, the cathodic reaction is the most rate limiting step in a MFC; therefore, efforts have been made to add photocatalyst in a cathodic reaction in order to continue

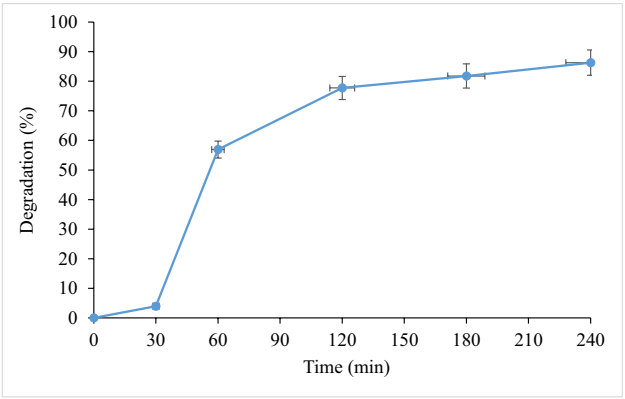

Fig. 5 Effect of time on photo-degradation of MB

the redox reaction. On the other hand, if anode is replaced with a photoanode (TiO_2), the power efficiency of MFC can be increased. Han et al. [32] have reported degradation of methyl orange (MO) dye at cathode in a MFC with an efficiency of 84.5 % over 36 h which was twice as done by carbon cathode electrode alone.

3.3.1 Effect of irradiation time

In photocatalytic degradation technique, UV radiation is required for photocatalytic activation. Thus, TiO_2 photocatalysts show low absorption in visible light and because of that efficiency of TiO_2 interrupts in natural sunlight. Light absorbing properties of TiO_2 can be spread by doping TiO_2 with metals. Correct doping can improve photo-reactivity of TiO_2 in both visible and UV light [33]. It is known that the concentration of irradiation time influences the photocatalytic performance of the samples. Figure 5 shows the effect of UV irradiation time on the spectra of MB solution. The degradation of MB increased with time increasing and reached about 86% degradation rate at 4 h. At the first 30 min, the MB-catalyst aqueous suspension was stirred in a dark place to ensure a homogenous mixture. However, about 4% of MB solution are degraded and it is expected the solution has been oxidized due to the surrounding factors. After 60 min of UV exposure, MB degradation increase tremendously and gradually increase up to 86%. This result inferred that catalyst has been activated upon UV irradiation and similar finding has also been reported by Koklic et al [34] and Wang et al. [23]. In general, the length of irradiation time is directly proportional to the percentage of methylene blue dye degradation. As the time increases, the degradation percentage also raises until it reaches an optimum value due to more hydroxyl radicals forming. By definition, the irradiation time in the photo-degradation process is the length of interaction between the photo catalyst and the inner rays to produce hydroxyl radicals, and the interaction between the

hydroxyl radicals and the substrate of organic compounds. Hydroxyl radicals are strong oxidizers used in degrading dye compounds, the more hydroxyl radicals formed the greater the percentage of degradation produced. This trend is likely keep increasing in longer irradiation times and influenced by other factors, such as dye concentration and surface area of the thin layer. According to Wardhani study [35], on the degradation of blue methylene compounds with TiO_2-zeolite photocatalysts, the longer the irradiation time, the greater the percentage of degradation obtained. Meanwhile, according to Permata, et al. [36], the percentage of degradation of phenol will increase with the duration of irradiation. So, it can be seen that the length of irradiation is directly proportional to the degradation of the substrate. Therefore, a higher irradiation time is needed to optimize the degradation percentage of dye significantly. In addition, this longer irradiation time may not be necessary for other pollutants or if using other photocatalysts.

3.3.2 Effect of amount of loaded catalyst

In order to avoid an ineffective excess of catalyst and to ensure a total absorption of efficient photons, the fitting mass of catalyst needed to be found. Figure 6 illustrates the photo-degradation of methylene blue with different amount of catalyst, 0.1 g/L, 0.3 g/L, 0.5 g/L, and 1.0 g/L. It can be seen that TiO_2 demonstrated superior photocatalytic activity for all different concentrations of catalyst. The photo-degradation of MB increased from 35.3 to 56.9% as the amount of catalyst increased from 0.1 up to 0.5 g/L confirming the heterogeneous nature of the photocatalytic process. This behavior can be associated to increased active sites available for MB dye molecule adsorption and degradation. However, further adding of loaded catalyst into MB solution changes the trend where the percentage of degradation reduces to 33.28%. This could be attributed to the deactivation of activated molecules by collision with ground-state molecules of TiO_2 [37]. Furthermore, in these conditions, particles tend to agglomerate, which makes a significant fraction of the catalyst to be inaccessible to either adsorbing the molecules or absorbing the radiation, with consequent decrease in the active sites available to the catalytic reaction. This finding can be explained using the mechanism of photo-degradation of MB in the presence of a catalyst as presented in the following reaction:

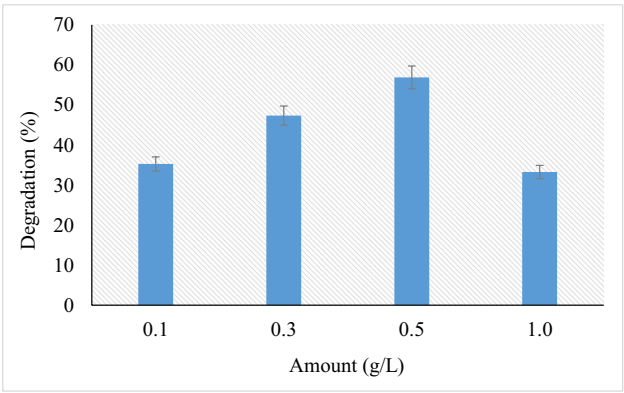

Fig. 6 Effect of amount of catalyst loading on photo-degradation of MB

$$\text{Catalyst} + h\upsilon(\text{UV}) \rightarrow \text{Catalyst}\left(e^-_{CB} + h^+_{VB}\right) \quad (2)$$

$$O_2 + e^-_{CB} \rightarrow O\cdot_2^- \quad (3)$$

$$H_2O + h^+_{VB} \rightarrow OH\cdot \quad (4)$$

$$MB^* + \text{catalyst} \rightarrow MB\cdot^+ + e^-_{CB}\,(\text{catalyst}) \quad (5)$$

$$MB\cdot^+ O\cdot_2^- \rightarrow \text{products} \quad (6)$$

$$MB\cdot^+ + OH\cdot \rightarrow \text{products} \quad (7)$$

As shown in the equation above, catalyst and MB undergo excitation and oxidation accordingly. Upon excitation, catalyst produce hole in the valence band and electron in the conduction band (Eq. 2). This electron-hole pairs thus allow the oxidation of MB on the surface of the catalyst (Eq. 3–5). The superoxide anion and hydroxyl radical then worked together to degrade MB (Eq. 6–7). After the loaded catalyst passes a certain level, the degradation of MB reduces due to the amount of MB is no longer sufficient to receive a photo-activated electron from the catalyst [23]. Fallowing this results, in the present case, 50 mg of catalyst is the maximum amount where the oxidation of 5 ppm MB can take place. Consequently, the unreacted electron will quickly have recombined forming many pairs of electron holes and hence decrease the percentage of degradation even more [38]. On one hand, higher TiO_2 concentration offers more reaction sites for oxidation of water molecules and production of hydroxyl radicals, thus increasing the reaction rate. On the other hand, TiO_2 also increases the light absorbance of the mixture, lowering the average light radiation and the total amount of photons received by the photocatalyst. The production rate of electron hole pairs is lowered, and thus fewer hydroxyl radicals are produced, decreasing the reaction rate. At lower TiO_2 concentration, the increasing effect dominates, while at higher TiO_2 concentration the latter decreasing effect plays a more important role. Therefore, the degradation speed would first increase and then decrease with increasing TiO_2 concentration [39].

3.4 Photocatalytic degradation of fungi Fusarium equiseti by TiO_2

Photocatalysis has also been shown to destroy microbial toxins. The ability to kill all other groups of microorganisms suggests that the surfaces have the potential to be self-sterilizing. Many studies have used pure cultures, although there are reports of photocatalytic activity against mixed cultures. The ability of the extracted catalyst to inhibit the growth of fungi is demonstrated in this section. A simple evaluation has been made on the inhibition of fungi using catalyst cultured on potato dextrose agar (PDA) plates. Figure 7(a) shows the growth of fungal strain A on the PDA plate that appeared as white-grayish-colored puffs. The microscopic image of fungal growth is shown in Fig. 7(b).

Further identification on the fungal strain was made using polymerized chain reaction (PCR) analysis. In order to confirm the species of fungal strain A, molecular characterization was performed and compared with the NCBI Nucleotide Collection Database. The phylogenetic tree was constructed based on the neighbor-joining method using Molecular Evolutionary Genetics Analysis 5 (MEGA5) for inducing the phylogeny or transformative relationship among other species and to develop branching tree dependent on their similitudes and contrasts in their characters. The sequence of PCR product and phylogenetic tree of fungus isolate strain A is depicted in the Figs. 8 and 9 accordingly. The 16S rRNA sequence data of the isolate fungal strain A was deposited into the Genbank database under the accession number of MZ960458. Sequence analysis of the ITS regions of the nuclear encoded rDNA showed significant alignment for *F. equiseti* with 100% identities. This phylogenetic tree helps in determining the similarity with other species and finding out their similarity and differences in the characters [40]. Figure 10 illustrates the observation made on the growth of fungi from 0 to 14 days with and without the presence of UV irradiation. The catalyst obtained from the previous experiment showed the maximum zone of inhibition against *F. equiseti.* The microbial effect of catalyst generally has been attributed to the decomposition of bacterial outer membranes by reactive oxygen species (ROS), primarily hydroxyl radicals (•OH), which leads to cell death [41]. An inhibition halo was clearly formed in the case of the samples coated with the TiO_2 and placed under UV light. This result could be attributed to the formation of oxidizing radicals, such as •OH or peroxides, capable of migrating to the culture medium and preventing the growth of the microorganisms, on and around it. According to our studies, the mechanism of cell death or inhibition of microorganism growth was still not elucidated. The most accepted mechanism for microorganism inactivation by ROS indicates that the •OH radicals or peroxides would initially promote the oxidation of the out membrane leading to a disorder in the cell permeability, even decomposition of the cell walls, and further oxidation of intracellular components that inhibit the cell respiration. The loss of the cell integrity could finally lead to the cell

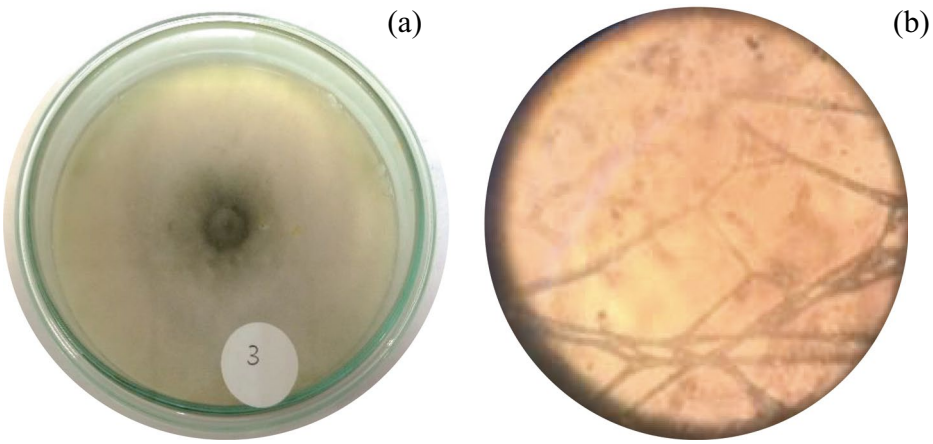

Fig. 7 **a** Macroscopic and (**b**) microscopic image of isolate wild fungi grown on PDA after 7 days at room temperature

Fig. 8 Sequence of PCR product of fungal strain A

```
>A, 547bp
TTCCGTAGGTGAACCTGCGGAGGGATCATTACCGAGTTTACAACTCCCAAACCCCTGTGAACATACCTATACGTTGCCTCGGCGGATC
AGCCCGCGCCCCGTAAAACGGGACGGCCCGCCCGAGGACCCCTAAACTCTGTTTTTAGTGGAACTTCTGAGTAAAACAAACAAATAAA
TCAAAACTTTCAACAACGGATCTCTTGGTTCTGGCATCGATGAAGAACGCAGCAAAATGCGATAAGTAATGTGAATTGCAGAATTCAG
TGAATCATCGAATCTTTGAACGCACATTGCGCCCGCCAGTATTCTGGCGGGCATGCCTGTTCGAGCGTCATTTCAACCCTCAAGCTCA
GCTTGGTGTTGGGACTCGCGGTAACCCGCGTTCCCCAAATCGATTGGCGGTCACGTCGAGCTTCCATAGCGTAGTAATCATACACCTC
GTTACTGGTAATCGTCGCGGCCACGCCGTAAAACCCCAACTTCTGAATGTTGACCTCGGATCAGGTAGGAATACCCGCTGAACTTAAG
CATATCAATAAGCGGAGGA
```

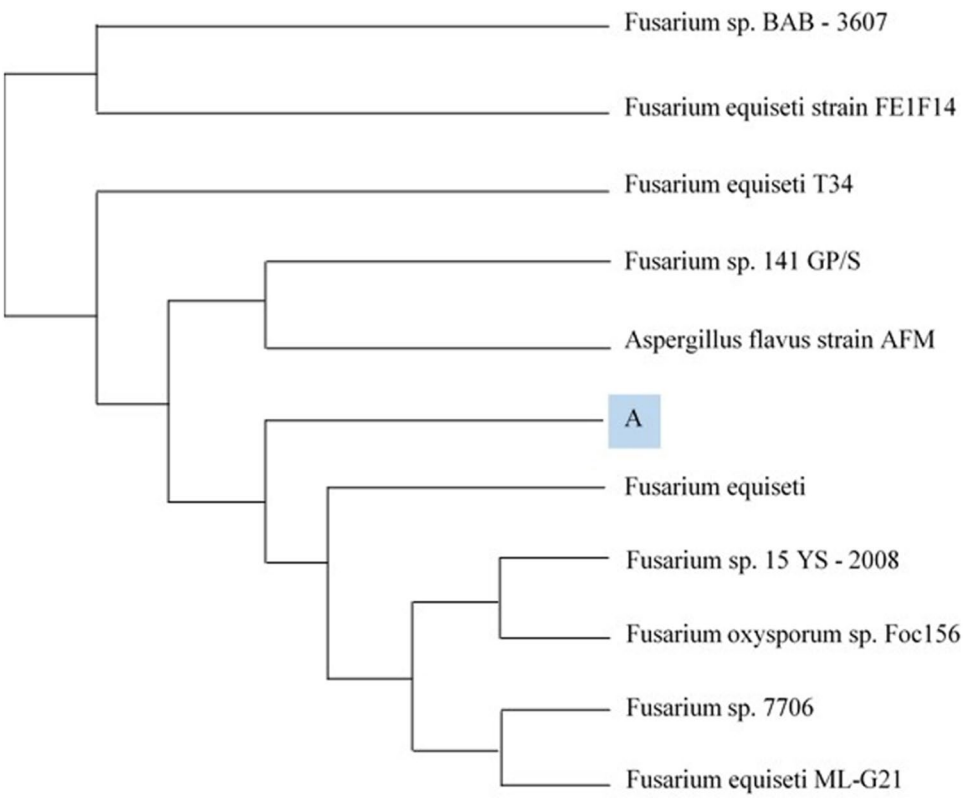

Fig. 9 Phylogenetic tree of fungus *F. equiseti*

death [42]. Another suggestion is that the •OH radicals are not the only species responsible for the biocide effect, i.e., the co-operative action can also promote peroxidation of phospholipid components of the lipid membrane, responsible for essential functions as respiratory activity and cell death. According to Tatlidil et al. [43], an Ag-TiO_2 catalyst was extremely active for the disinfection of *Candida albicans* even under dark conditions [43]. In another study, the disinfection of *Fusarium solani* spores were carried out by Polo-López et al. [44]. Our results are in agreement with the previous work by Reddy et al. [45]. Their study reported that the solar light-only (no TiO_2) disinfection of *Fusarium* required a high UVA dose and UVA intensity, whereas in the presence of TiO_2 the required UVA dose or intensity was very low. Fungal spores were generally more resistant than vegetative forms, and *Trichoderma harzianum* spores in particular were resistant to killing under the conditions tested [46]. Cysts of *Acanthamoeba* showed only a 50% reduction during the treatment time and may have been killed if the treatment time had been extended [47].

4 Conclusions

The leached sulfate solution containing dissolved metal ions mainly Ti ions, Al ions, and Fe ions subjected to solvent extraction using Cyanex 272 follows the order of Ti > Al > Fe. The precipitated and calcinated, the final product (TiO_2) was a brownish-white color powder form. The purity of the recovered TiO_2 with respect to other impurities was around 70.8%. It was estimated that the final ratio of TiO_2:Al_2O_3:Fe_2O_3 was 81:11:8 accordingly. XRD analysis showed six distinct diffraction peaks which attributed to the crystallized phase of TiO_2 anatase with a minor constituent of Fe_2O_3 hematite and Al_2O_3. The FESEM image also showed that the micrometer-sized grain aggregates presence in the form of uniformed spherical shape with considerable variation of particle size. The photocatalytic activity of recovered TiO_2 was investigated against methylene blue and isolated fungi. The photo-degradation of methylene blue increased with a longer duration and reached about 86% degradation rate after 4 h. The increased in the amount of TiO_2 from 0.1 to 0.5 g/L resulted in higher degradation of methylene blue from 35.3 to 56.9%. However, further added of loaded TiO_2 into methylene blue solution changes the trend where percentage of degradation reduced to 33.28%. In order to test the inactivation of *Fusarium equiseti* under the presence of UV light irradiation, 0.5 g/L of TiO_2 was loaded into the PDA medium. The finding showed that almost 50% of the fungi growth was inhibited in the duration of 14 days. In contrast, zero inhibition of fungi growth was detected without the presence of loaded TiO_2. It should be mentioned that TiO_2 is generally a challenging substance to leach due to its stable nature; hence, the selection of the

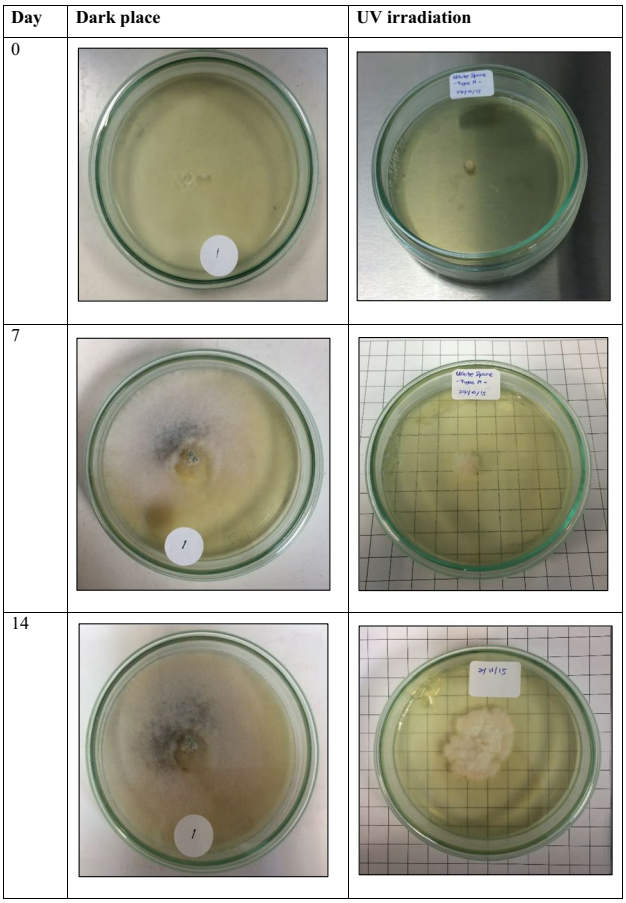

Fig. 10 Observation on the growth of fungi in dark place and with the presence of UV irradiation

leaching reagent should be considered carefully. In order to improve the extraction efficiency of metals, selection of extractant, initial concentration of sulfate leached solution and pH should be takes into consideration. In addition, further investigation on the recovery of valuable of metals from other secondary sources is suggested.

Funding This research is financially supported by PDRU Grant- Vot No. Q.J130000.21A2.04E53, Hitachi Global Foundation, MRUN R.J130000.7805.4L886, and Research University Grant Scheme (Vote Q.J130000.2609.09J40) which are gratefully acknowledged.

References

1. Walia K (2019) Global titanium dioxide market analysis report 2018–2025. Value Market Research, Pune
2. He R, Huang X, Zhang J, Geng Y, Guo H (2019) Preparation and evaluation of exhaust-purifying cement concrete employing titanium dioxide. Materials 12(13):2182. https://doi.org/10.3390/ma12132182
3. Nakahara K, Muttakin M, Yamamoto K, Ito K (2020) Computational fluid dynamics modelling of the visible light photocatalytic oxidation process of toluene for indoor building materials with locally doped titanium dioxide. Indoor Built Environ 29(2):163–179. https://doi.org/10.1177/1420326X19854499
4. Areerachakul N, Sakulkhaemaruethai S, Johir MAH, Kandasamy J, Vigneswaran S (2019) Photocatalytic degradation of organic pollutants from wastewater using aluminium doped titanium dioxide. J Water Process Eng 27:177–184. https://doi.org/10.1016/j.jwpe.2018.12.006
5. Varjani S, Rakholiya P, Shindhal T, Shah AV, Ngo HH (2021) Trends in dye industry effluent treatment and recovery of value added products. J Water Process Eng 39:101734. https://doi.org/10.1016/j.ibiod.2008.10.002
6. Shindhal T, Rakholiya P, Varjani S, Pandey A, Ngo HH, Guo W, Taherzadeh MJ (2021) A critical review on advances in the practices and perspectives for the treatment of dye industry wastewater. Bioengineered 12(1):70–87. https://doi.org/10.1080/21655979.2020.1863034
7. Varjani S, Rakholiya P, Shindhal T, Shah AV, Ngo HH (2021) Trends in dye industry effluent treatment and recovery of value added products. J Water Process Eng 39:101734. https://doi.org/10.1016/j.jwpe.2020.101734
8. Kumar PS, Varjani SJ, Suganya S (2018) Treatment of dye wastewater using an ultrasonic aided nanoparticle stacked activated carbon: kinetic and isotherm modelling. Bioresource Technol 250:716–722. https://doi.org/10.1016/j.biortech.2017.11.097
9. Waghmode MS, Gunjal AB, Mulla JA, Patil NN, Nawani NN (2019) Studies on the titanium dioxide nanoparticles: biosynthesis, applications and remediation. SN Appl Sci 1(4):1–9. https://doi.org/10.1007/s42452-019-0337-3
10. Zhu X, Pathakoti K, Hwang HM (2019) Green synthesis of titanium dioxide and zinc oxide nanoparticles and their usage for antimicrobial applications and environmental remediation. In Green Synthesis Charact Appl Nanoparticles 223-263. https://doi.org/10.1016/B978-0-08-102579-6.00010-1
11. Parham HF, Ishak NH, Hassan ZFA (2018) Mold growth risk in a newly built hospital building in Malaysia–problems and solutions. J Design Built Environ:16–25 https://doi.org/12155-13-23792-2-10-20180725
12. Zabka M, Pavela R (2018) Review Chapter: Fusarium genus and essential oils. In: Natural Antimicrobial Agents. Springer, Cham, pp 95–120. https://doi.org/10.1007/978-3-319-67045-4_5
13. Babaizadeh H, Hassan M (2013) Life cycle assessment of nano-sized titanium dioxide coating on residential windows. Construct Build Mater 40:314–321. https://doi.org/10.1016/j.conbuildmat.2012.09.083
14. Saravanan A, Karishma S, Kumar PS, Varjani S, Yaashikaa PR, Jeevanantham S, Reshma B (2021) Simultaneous removal of Cu (II) and reactive green 6 dye from wastewater using immobilized mixed fungal biomass and its recovery. Chemosphere 271:129519. https://doi.org/10.1016/j.chemosphere.2020.129519
15. Krishnan S, Zulkapli NS, Din MFM, Abd Majid Z, Honda M, Ichikawa Y, Guntor NAA (2020) Statistical optimization of titanium recovery from drinking water treatment residue using response surface methodology. J Environ Manag 255:109890. https://doi.org/10.1016/j.jenvman.2019.109890
16. Chen Z, You Y, Morita K (2018) Synthesis and kinetics of titanium silicides from photovoltaic industry waste and steelmaking slag for silicon and titanium recovery. ACS Sustainable Chem Eng 6(5):7078–7085. https://doi.org/10.1021/acssuschemeng.8b00919
17. Junior ABB, Costa RH, Espinosa DCR, Tenório JAS (2019) Recovery of scandium by leaching process from Brazilian red mud. In: Rare Metal Technology. Springer, Cham, pp 73–79. https://doi.org/10.1007/978-3-030-05740-4_8

18. Begum N, Khuzaima N, Ching FF, Bari M, Rezan S (2016) Characterization of Langkawi black sand for the recovery of titanium. In Key Engineering Materials 709:70-73 Trans. Tech Publications Ltd. https://doi.org/10.4028/www.scientific.net/KEM.709.70
19. Che Jamin N, Mahmood NZ (2015) Scheduled waste management in Malaysia: an overview. In Advanced Materials Research 1113:841-846. Trans Tech Publications Ltd. https://doi.org/10.4028/www.scientific.net/AMR.1113.841
20. Zhu Z, Zhang W, Cheng CY (2011) A literature review of titanium solvent extraction in chloride media. Hydrometallurgy 105(3-4):304–313. https://doi.org/10.1016/j.hydromet.2010.11.006
21. Gao LK, Rao B, Dai HX, Hong Z, Xie HY (2019) Separation and extraction of scandium and titanium from a refractory anatase lixivium by solvent extraction with D2EHPA and primary amine N1923. J Chem Eng Japan 52(11):822–828. https://doi.org/10.1252/jcej.18we347
22. Musariri B, Akdogan G, Dorfling C, Bradshaw S (2019) Evaluating organic acids as alternative leaching reagents for metal recovery from lithium ion batteries. Min Eng 137:108–117. https://doi.org/10.1016/j.mineng.2019.03.027
23. Wang J, Li C, Zhuang H, Zhang J (2013) Photocatalytic degradation of methylene blue and inactivation of Gram-negative bacteria by TiO_2 nanoparticles in aqueous suspension. Food Control 34(2):372–377. https://doi.org/10.1016/j.foodcont.2013.04.046
24. Abiola ON (2019) Polymers for coagulation and flocculation in water treatment. In: Polymeric materials for clean water. Springer, Cham, pp 77–92. https://doi.org/10.1007/978-3-030-00743-0_4
25. Kleemann N, Torres DP, Ribeiro AS, Bamberg AL (2020) Cold finger with semi closed reflux system for sample preparation aiming at Al, Ca, Cr, Cu, Fe, K, Mg, Mn, Ni, V and Zn determination in drinking water treatment sludge by MIP OES. Analytica Chimica Acta 1096:9–17. https://doi.org/10.1016/j.aca.2019.10.064
26. Gomes SDC, Zhou JL, Li W, Long G (2019) Progress in manufacture and properties of construction materials incorporating water treatment sludge: a review. Resources Conserv Recycl 145:148–159. https://doi.org/10.1016/j.resconrec.2019.02.032
27. Aphairaj D, Wirunmongkol T, Pavasupree S, Limsuwan P (2011) Effect of calcination temperatures on structures of TiO_2 powders prepared by hydrothermal method using Thai leucoxene mineral. Energy Procedia 9:539–544. https://doi.org/10.1016/j.egypro.2011.09.062
28. Covei M, Perniu D, Bogatu C, Duta A (2019) CZTS-TiO_2 thin film heterostructures for advanced photocatalytic wastewater treatment. Catalysis Today 321:172–177. https://doi.org/10.1016/j.cattod.2017.12.003
29. Le HA, Chin S, Jurng J (2012) Photocatalytic degradation of methylene blue by a combination of TiO_2-anatase and coconut shell activated carbon. Powder Technol 225:167–175. https://doi.org/10.1016/j.powtec.2012.04.004
30. Alakhras F, Alhajri E, Haounati R, Ouachtak H, Addi AA, Saleh TA (2020) A comparative study of photocatalytic degradation of Rhodamine B using natural-based zeolite composites. Surfaces Interfaces 20:100611. https://doi.org/10.1016/j.surfin.2020.100611
31. Vinayak V, Khan MJ, Varjani S, Saratale GD, Saratale RG, Bhatia SK (2021) Microbial fuel cells for remediation of environmental pollutants and value addition: special focus on coupling diatom microbial fuel cells with photocatalytic and photoelectric fuel cells. J Biotechnol. https://doi.org/10.1016/j.jbiotec.2021.07.003
32. Han HX, Shi C, Yuan L, Sheng GP (2017) Enhancement of methyl orange degradation and power generation in a photoelectrocatalytic microbial fuel cell. Appl Energy 204:382–389. https://doi.org/10.1016/j.apenergy.2017.07.032
33. Riaz N, Chong FK, Man ZB, Sarwar R, Farooq U, Khan A, Khan MS (2016) Preparation, characterization and application of Cu–Ni/TiO_2 in Orange II photodegradation under visible light: effect of different reaction parameters and optimization. RSC Advances 6(60):55650–55665. https://doi.org/10.1039/C6RA10371E
34. Koklic T, Pintarič Š, Zdovc I, Golob M, Umek P, Mehle A, Štrancar J (2018) Photocatalytic disinfection of surfaces with copper doped TiO_2 nanotube coatings illuminated by ceiling mounted fluorescent light. Plos One 13(5):e0197308. https://doi.org/10.1371/journal.pone.0197308
35. Wardhani S, Purwonugroho D, Fitri CW, Prananto YP (2018) Effect of pH and irradiation time on TiO_2-chitosan activity for phenol photo-degradation. In AIP Conference Proceedings 050009. AIP Publishing LLC. https://doi.org/10.1063/1.5062759
36. Permata DG, Diantariani NP, Widihati IAG (2015) Degradasi fotokatalitik fenol menggunakan fotokatalis ZnO dan sinar UV. Universitas Udayana, Bali
37. Matsunami D, Yamanaka K, Mizoguchi T, Kojima K (2019) Comparison of photodegradation of methylene blue using various TiO_2 films and WO_3 powders under ultraviolet and visible-light irradiation. J Photochem Photobiol A: Chem 369:106–114. https://doi.org/10.1016/j.jphotochem.2018.10.020
38. Robert J, Jüstel T, Ulber R, Jordan V (2018) Catalyst deactivation during photocatalytic degradation of methylene blue with TiO_2. Chemie Ingenieur Technik 90(5):643–652. https://doi.org/10.1002/cite.201700144
39. Xu C, Rangaiah GP, Zhao XS (2014) Photocatalytic degradation of methylene blue by titanium dioxide: experimental and modeling study. Indust Eng Chem Res 53(38):14641–14649
40. Yaashikaa PR, Senthil Kumar P, Varjani S, Saravanan A (2020) Rhizoremediation of Cu (II) ions from contaminated soil using plant growth promoting bacteria: an outlook on pyrolysis conditions on plant residues for methylene orange dye biosorption. Bioengineered 11(1):175–187. https://doi.org/10.1080/21655979.2020.1728034
41. Jayaseelan C, Rahuman AA, Roopan SM, Kirthi AV, Venkatesan J, Kim SK, Siva C (2013) Biological approach to synthesize TiO_2 nanoparticles using Aeromonas hydrophila and its antibacterial activity. Spectrochimica Acta Part A: Mol Biomol Spectros 107:82–89. https://doi.org/10.1016/j.saa.2012.12.083
42. Harandi D, Ahmadi H, Achachluei MM (2016) Comparison of TiO_2 and ZnO nanoparticles for the improvement of consolidated wood with polyvinyl butyral against white rot. Int Biodeterioration Biodegradation 108:142–148. https://doi.org/10.1016/j.ibiod.2015.12.017
43. Tatlıdil İ, Sökmen M, Breen C, Clegg F, Buruk CK, Bacaksız E (2011) Degradation of *C andida albicans* on TiO_2 and Ag-TiO_2 thin films prepared by sol–gel and nanosuspensions. J sol-gel Sci Technol 60(1):3–32. https://doi.org/10.1007/s10971-011-2546-0
44. Polo-López MI, García-Fernández I, Oller I, Fernández-Ibáñez P (2011) Solar disinfection of fungal spores in water aided by low concentrations of hydrogen peroxide. Photochem Photobiol Sci 10(3):381–388. https://doi.org/10.1039/C0PP00174K
45. Reddy PVL, Kavitha B, Reddy PAK, Kim KH (2017) TiO_2-based photocatalytic disinfection of microbes in aqueous media: a review. Environ Res 154:296–303. https://doi.org/10.1016/j.envres.2017.01.018
46. Giannantonio DJ, Kurth JC, Kurtis KE, Sobecky PA (2009) Effects of concrete properties and nutrients on fungal colonization and fouling. Int Biodeterioration Biodegradation 63(3):252–259. https://doi.org/10.1016/j.ibiod.2008.10.002
47. Sokmen M, Degerli S, Aslan A (2008) Photocatalytic disinfection of *Giardia intestinalis* and *Acanthamoeba castellani* cysts in water. Exp Parasitol 119(1):44–48. https://doi.org/10.1016/j.exppara.2007.12.014